Available on CMS information server

CMS NOTE 1997/063

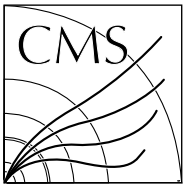

The Compact Muon Solenoid Experiment

CMS Note

Mailing address: CMS CERN, CH-1211 GENEVA 23, Switzerland

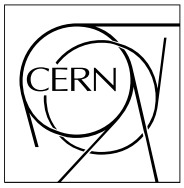

July 10, 1997

Beam test performance of a closed microstrip gas chamber module for the CMS forward tracker

S. Bachmann, F. Beißel, C. Camps, V. Commichau, G. Flügge, K. Hangarter, J. Kremp, D. Macke, M. Petertill, O. Pooth, R. Schulte, H. Szczesny, M. Tonutti

III. Physikalisches Institut, RWTH Aachen

Abstract

We built and tested a closed MSGC module for the CMS forward tracker with trapezoidal strip patterns on 300 μm DESAG263 glass substrates produced by OPTIMASK. In the 100 GeV X5 μ–beam at CERN, we investigated the behaviour of this module foreseen for four wedge shaped substrates, 512 anode strips each.

Good separation of signal and noise was achieved and efficiencies reached 97%. The variation of gain across the strip pattern was examined.

1 Introduction

Microstrip gas chambers (MSGCs) [1, p.28] are foreseen to set up the outer layers of the inner tracking system in CMS [1]. Since their introduction by A. Oed [2] they have attracted a lot of interest due to good position– and two-track resolution, high rate capability and lower costs compared to silicon detectors.

In this note we concentrate on the mechanical setup of an MSGC module designed for the CMS forward tracker. Therefore we used trapezoidal strip patterns on wegde shaped glass substrates and built a banana–shaped detector module (mechanical mock-up shown in Fig. 1).

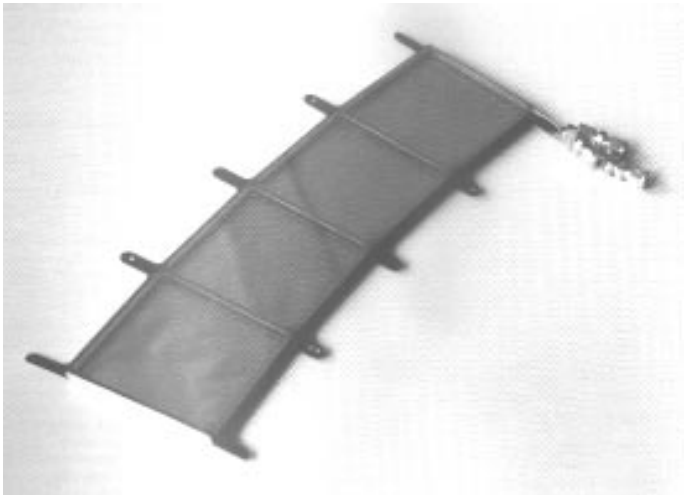

Figure 1: Closed module design.

2 Closed MSGC modules

2.1 Concept

To achieve protection of the delicate substrate surfaces, the detection volume is closed at an early construction stage before mounting of the electronics and bonding. Pressure differences across the fragile substrates and drift cathodes are prevented by a gas flow through the module as shown in Fig. 2. The closed concept foresees front end

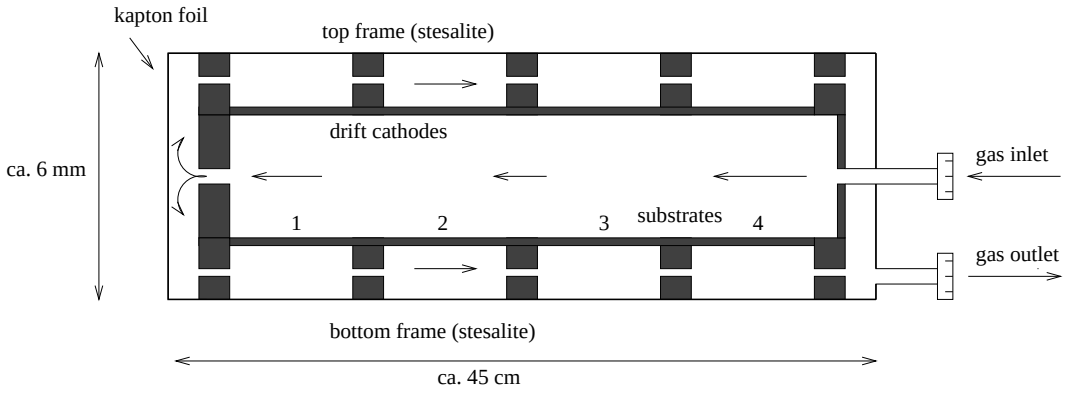

Figure 2: Gas flow through the module.

electronics and HV hybrids outside the detector volume to avoid undesired gas pollution by critical materials. To align the modules on the CMS forward wheel structure, fiducal marks in the frames are provided.

The components from bottom to top:

metallized kapton foil	closes the module and provides electric shielding
bottom frame	holds the substrates and defines the volume to avoid pressure differences
four substrates	trapezoidal metal strips on glass
spacer frame	defines the sensitive detector volume
drift cathodes	metallized glass
top frame	volume to avoid pressure differences on the drift cathodes
metallized kapton foil	closes the module

2.2 The prototype module

2.2.1 Components

In the prototype module we used 2 substrates and 2 dummy glass plates to test the basic features of the design. The wedge shaped strip pattern of aluminium anodes and cathodes is manufactured on 300 μm thick DESAG263 glass[1)] by OPTIMASK[2)]. All 512 anodes have a constant width of 10 μm and the inter-anode pitch varies from 180 μm (short base) to 200 μm (long base). The cathode width changes from 85 μm to 100 μm considering

$$\text{distance between anode and cathode} = 20\ \mu\text{m} + \text{pitch} / 8, \qquad [1, \text{p.29}]$$

which is the result of field calculations. This provides an electric field that offers a similar gas amplification over the full strip length, so no position dependence of the signal amplitude should occur.

The substrates, originally developed for another module concept [3], are not suited for the closed design: the spacer frame had to be glued across adjacent anodes and cathodes due to the only 200 μm short bonding pads which need to have a certain distance to the frame in order to provide enough working space for bonding. After the bonding procedure the region of anodes and cathodes outside the gas volume has to be insulated with silicon gel to avoid discharges.

To overcome this problem, the closed design needs $\sim$ 6 mm long bonding pads, so that the frame can be glued across the bonding pads, and the whole pattern of anodes and cathodes is located inside the detection volume.

2.2.2 Mounting

Cleaning of all items is done in an ultrasonic bath filled with deionized water. The components are glued together under clean–room conditions in a flow box, using HEXEL EPO 93/L [4], a room temperature curing epoxy that shows no outgasing in Argon and Dimethylether. This also applies to the frames made of Stesalit[3)]. During the assembly of this prototype module we did not use an aligning tool to adjust the substrates one to another.

To ensure a homogenous gas distribution inside the module, a strip of kapton foil with small holes is glued over a groove milled into one side of the spacer frame (Fig. 3).

The substrates and drift cathodes are glued to the bottom frame (Fig. 4) and the top frame respectively. The detection volume is closed by glueing together all three parts. Finally, metallized kapton foils close the volumes that avoid pressure differences across drift cathodes and substrates. Fig. 5 shows a picture of the assembled module.

2.2.3 Readout electronics and HV supply

The PreMux128 chip [5] is used as front end electronics, and two hybrids (each containing four chips and a pitch adaptor mounted on a ceramic carrier) were bonded to the 1024 anode strips. The HV connection is provided by adapter circuit boards with 1 MΩ resistors for each group of 16 cathode strips, preceded by a common 1 MΩ protection resistor to limit the current in case of discharges. Conductive silver connects the cathode groups on the substrates to the circuit boards.

---

1) high resistivity boro–silicate glass manufactured by Deutsche Spezialglas AG

2) Paris, France

3) Stesalit AG, Zullwil, Switzerland

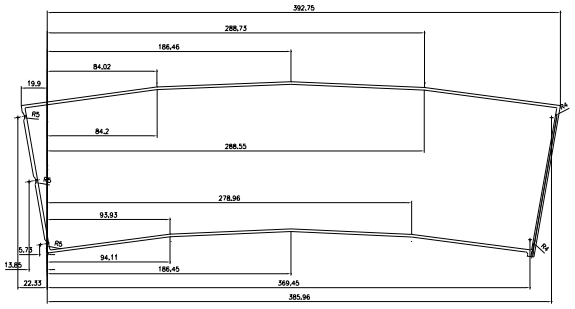

Figure 3: Spacer frame: defines the detection volume.

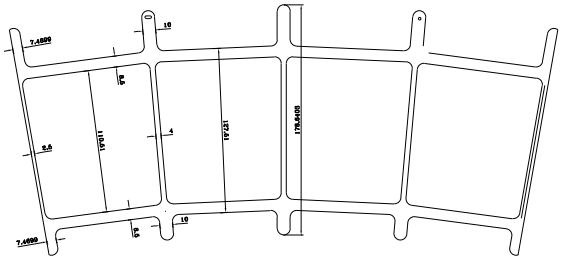

Figure 4: Bottom frame: holds the substrates.

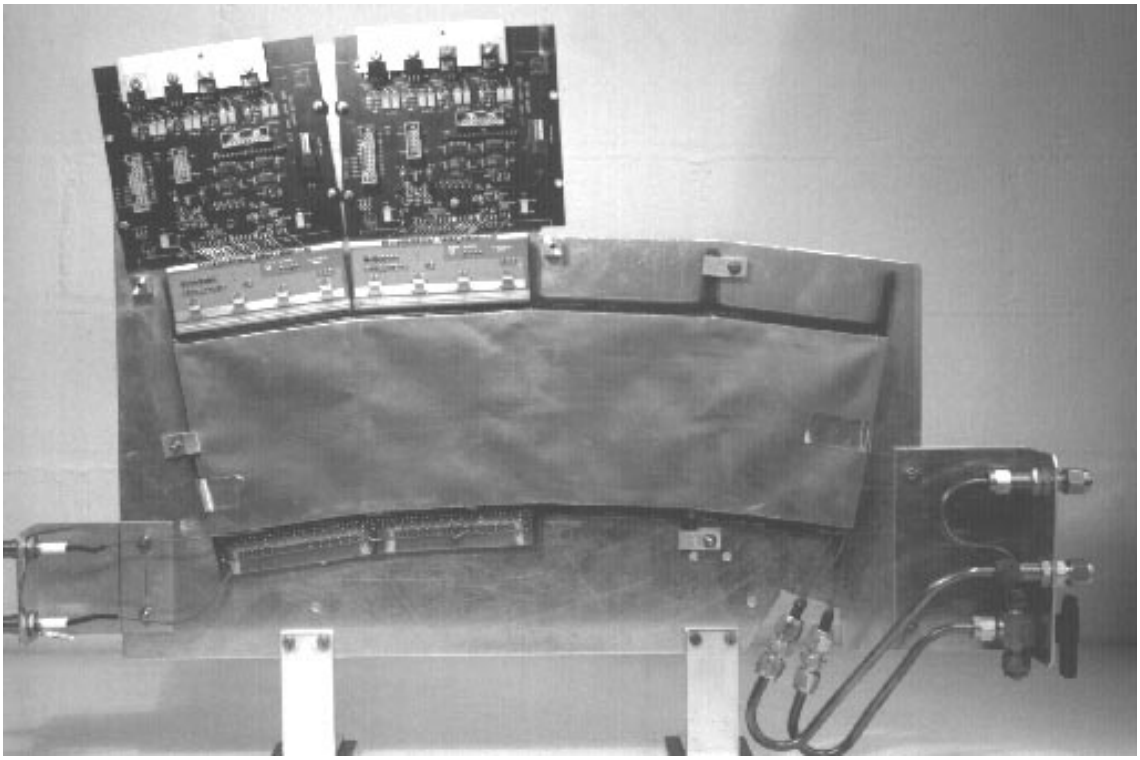

Figure 5: The prototype module. On the left side from bottom to top: HV supply, substrates in the frame, PreMux128 hybrids, motherboards. On the right side: gas in– and outlet.

Due to shorts, only 52 out of 64 cathode groups could be connected to HV. This corresponds to 832 strips. In 10 of these groups we can determine the short–causing strip precisely, so that a reactivation may be possible by removing single bondings without opening the detector module.

To read out the PreMux128 chip we used a CAMAC based DAQ system. Fig. 6 shows the components. The PreMux128 motherboards [6] are connected to an adapterboard [7] that generates a fast trigger after particle transition, detected by a coincidence of up to four scintillators. The readout sequence [8] is started and the multiplexed analogue signals are digitized by ADCs [9] with a resolution of 8 bits. A programmable pulse generator [10] provides test pulses with adjustable amplitude and timing. For more detailed information of the PreMux128 readout see [11].

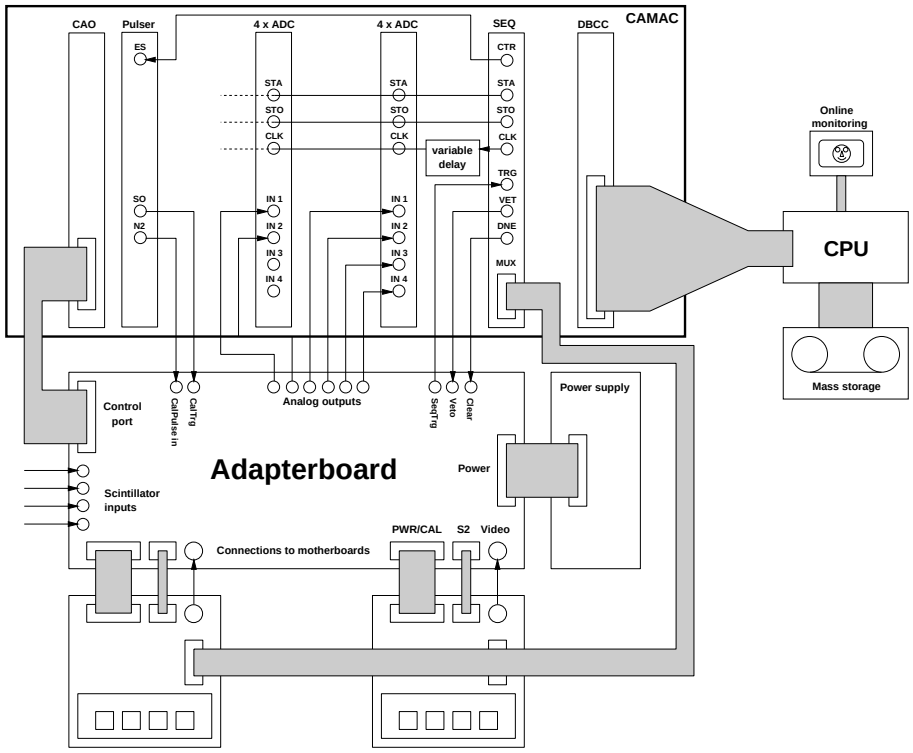

Figure 6: Readout system overview. CAO: CAMAC output register to control the adapterboard, SEQ: Sequencer to generate readout control signals, DBCC: CAMAC crate controller.

3 Experimental setup

With the X5 beam [12], CERN provides a test facility with electrons, pions and muons in an energy range up to 250 GeV. All results were obtained with a 100 GeV muon beam.

This beam could irradiate one of the substrates in the module entirely. To provide fast trigger signals, two scintillators with an area of 10×10 cm^2 and 2×2 cm^2 were connected to the adapterboard. The scintillators could be used with or without coincidence. Installation of the module was done on an optical bench together with four 10×10 cm^2 MSGCs and two neutron–irradiated silicon detectors. An open gas system was used to deliver Ar/DME (1/2) or Ne/DME (1/2).

As the X5 beam runs in spill mode we got $\sim$ 10 000 particles in 2.45 s every 14.4 s. In total, 4096 channels were read out with a rate of $\sim$ 100 triggers/spill. We stored 3.6×10^6 events during 11 days of operation.

4 Data processing

The raw data were displayed on screen as shown in Fig. 7. All PreMux128 readout parameters are remote controlled by the online software [13], which allows to take a sampling point variation curve, gain measurement for all PreMux128 channels, hitmap taking and pedestal correction. The shape of the hitmap in Fig. 8 represents the

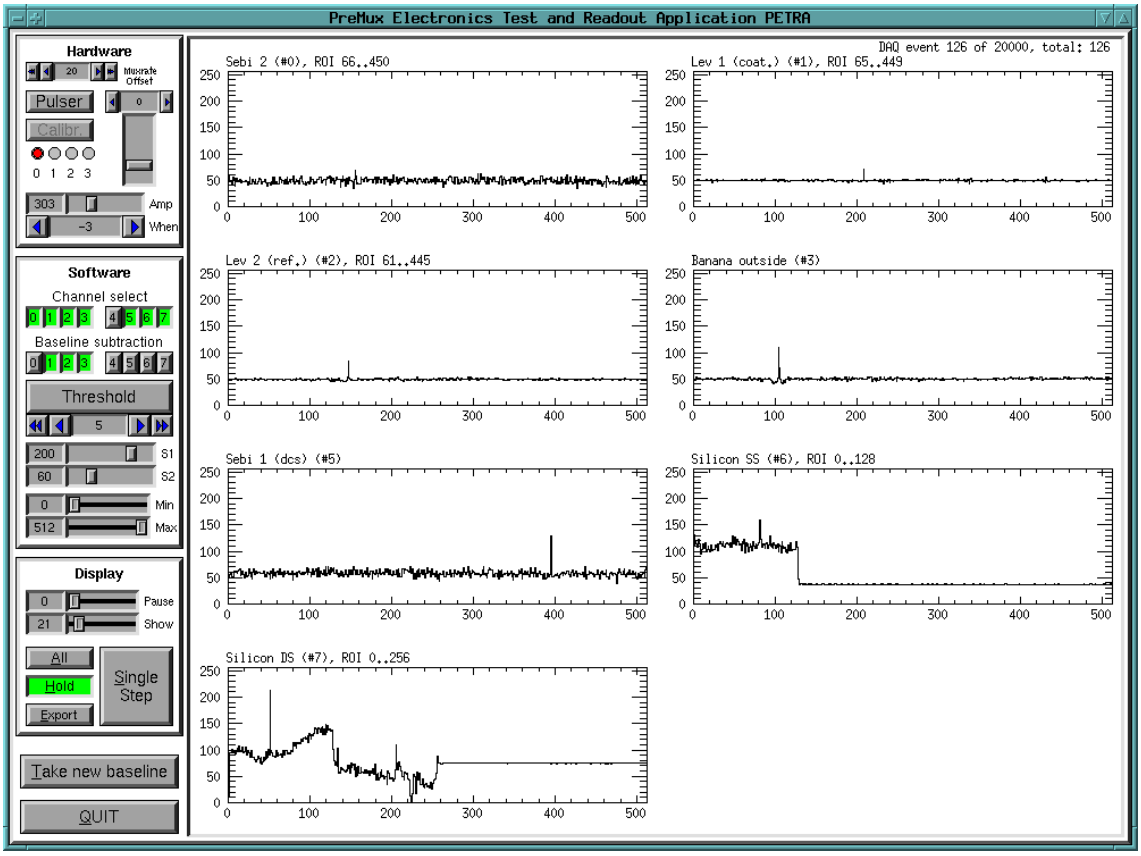

Figure 7: A screenshot of the online display. The small window labeled as ”Banana outside” shows the response of the module’s outer substrate to an incident particle.

area of the small scintillator. In this region of 2 cm width ($\sim$100 strips) we observed 6 broken anodes and their effect on neighbouring strips, showing more entries due to the fact that their acceptance region has grown.

4.1 Raw data correction

The retrieval of the particle related information from the raw data requires a compensation of the signal distortions caused by the electronics.

Every channel has its own pedestal, which is the amplitude of the output signal without applied charge. It varies between the channels.

Furthermore, there are shifts common to all channels on a chip (common mode). The electronics attached to the detector was operated in a single point sampling mode, triggered by particle transition. Each PreMux128 contains 129 preamplifier-shaper units, from which one is not connected to an input pad. Subtraction of this ”dummy channel” signal should compensate most of the common mode caused by altering working conditions of the chip (e.g. temperature and operating voltages).

The raw data amplitude $r_{i,j}$ for event i and channel j is therefore given by

$$r_{i,j} = d_{i,j} + p_j + c_i + n_{i,j},$$

where $d_{i,j}$ is the data signal, p_j the pedestal value for channel j, c_i the common mode for event i and $n_{i,j}$ the electronic noise.

In a first step, each channel data is corrected for its pedestal value, which may be derived from a large sample of readouts without particles ($d_{i,j} = 0$). Because common mode and noise are symmetric with respect to the pedestal, they vanish when calculating the mean value for N events:

$$p_j = \frac{1}{N} \sum_{i=1}^{N} r_{i,j}.$$

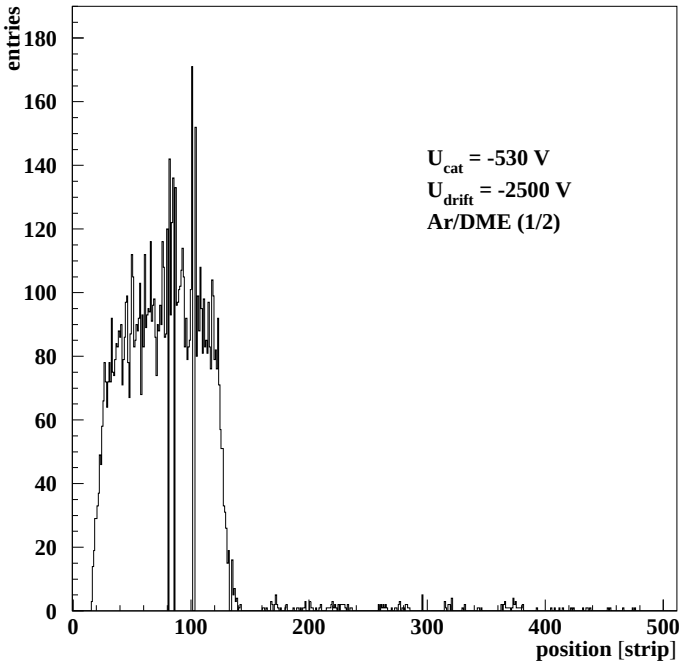

Figure 8: Hitmap (position of maximum entry for each event).

After application of the pedestal correction, it is necessary to compensate common mode shifts that are not eliminated by the dummy channel subtraction. These may be related to environmental electric fields picked up by all channels. As seen in Fig. 9, the effect differs from chip to chip.

This correction is done for each chip and event, calculating the mean value for all channels that have not seen a hit (channel exceeding a certain threshold):

$$d_{i,j} = r_{i,j} - p_j - \underbrace{\frac{1}{N_{no\ hit}} \sum_{\substack{j=1 \\ no\ hit}}^{chan.} (r_{i,j} - p_j)}_{c_i} .$$

The noise $n_{i,j}$ will always remain as a part of the data.

4.2 Cluster finding

Usually, the charge produced in an MSGC spreads over more than one strip, so a single particle generates a cluster, i.e. signals on adjacent strips. The search for these clusters starts with the tagging of strips that are candidates for cluster contributors.

This decision is based on a threshold calculated individually for each channel, which takes the different noise mean values σ_j into account. They may also be derived from pedestal data according to

$$\sigma_j = \sqrt{\frac{\sum_{i=1}^{N} (r_{i,j} - p_j - c_i)^2}{N}}.$$

A cluster is defined as a group of adjacent strips, each exceeding its pedestal value by more than $2.5\sigma_j$. The resulting cluster parameters (height, width and charge) are given in Fig. 10.

The SNR for the cluster in event i may be calculated dividing the cluster charge by the gaussian sum of the noise from the contributing channels:

$$SNR_i = \frac{\sum_{j=m}^{n} d_{i,j}}{\sqrt{\sum_{j=m}^{n} {\sigma_j}^2}},$$

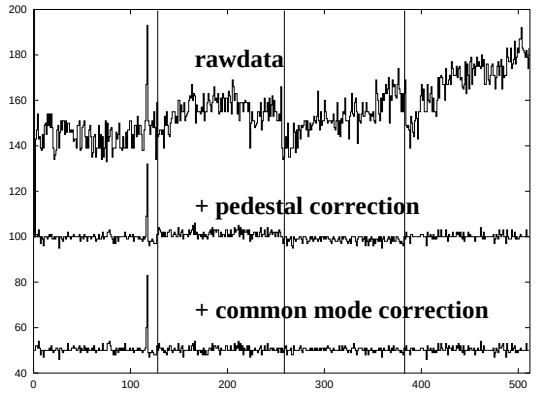

Figure 9: Correction of raw data for pedestals and common mode. Vertical lines show the chip borders.

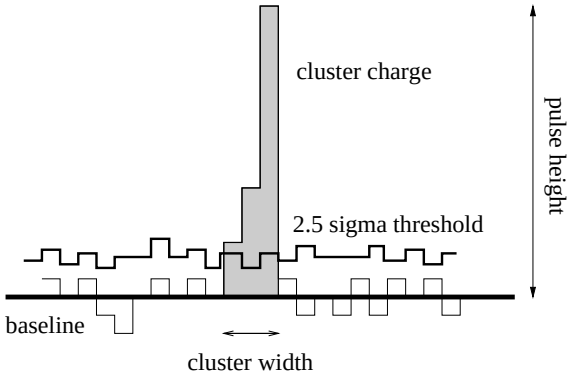

Figure 10: Definition of cluster parameters.

where m and n denote first and last channel of the cluster respectively.

4.3 Results

The cluster charge is proportional to the energy deposition in the chamber volume. Fig. 11 shows the distribution filled with 10 000 events, where the only applied cut is the channel threshold described above and only the biggest cluster is taken into account.

To eliminate the noise peak, which is the result of chamber inefficiencies, the introduction of a second threshold is necessary. We choose a cut on the pulse height (Fig. 12).

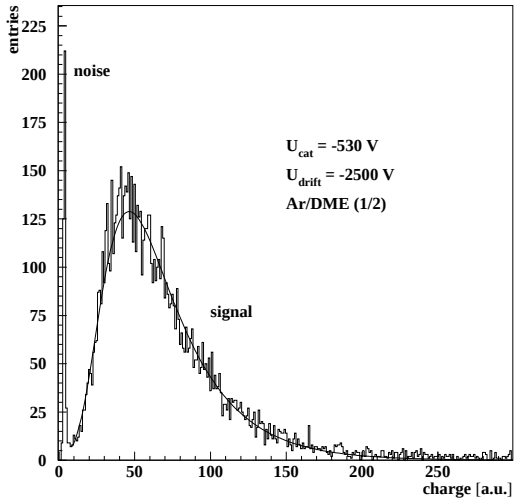

Figure 11: Cluster charge distribution with noise peak and fitted landau lineshape.

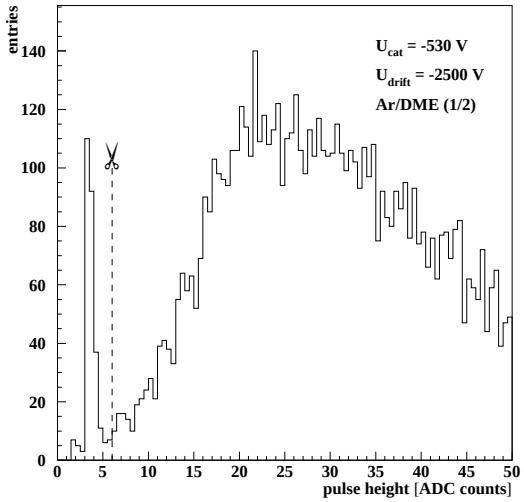

Figure 12: Distribution of the pulse height to determine the cut parameter.

Fig. 13 gives the SNR distribution of the selected events. The COG of this histogram may now represent the SNR of the chamber,

$$\overline{SNR} = \frac{1}{N_{hit}} \sum_{\substack{i=1 \\ hit}}^{N} SNR_i,$$

which is plotted against the cathode voltage in Fig. 14.

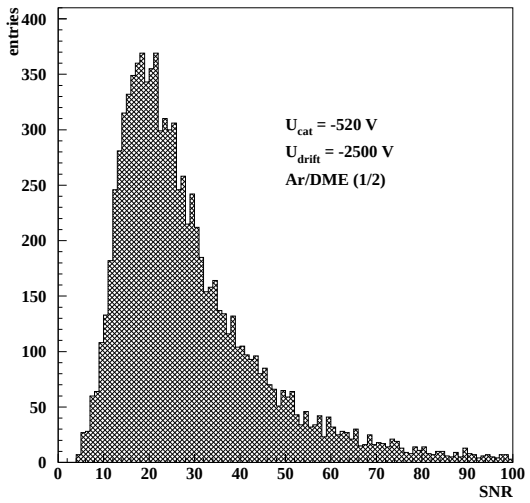

Figure 13: SNR distribution after pulse height cut.

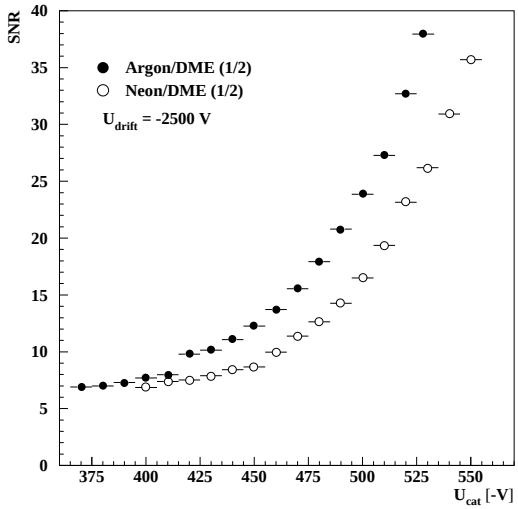

Figure 14: Behaviour of the SNR versus cathode voltage for two gas mixtures.

To achieve information concerning the efficiency of the detector, we compared the number of events passing the pulse height criterion with respect to the number of triggers. This ratio is defined as efficiency and shown in Fig. 15.

4.4 Variation of the gain along and perpendicular to the strips

On the optical bench, the detector module was mounted with clamps. It was possible to shift it with respect to the trigger region defined by the 2×2 cm^2 scintillator.

Fig. 16 shows the effect of the varying pitch to the SNR, analyzed for three regions of strips. The results do not indicate a clear tendency, but the fluctuations are below 30% in the worst case and below 6% along the same group of strips. It is important to remark that due to the fact there were HV groups not connected, only a fraction of the 100 strips covered by the scintillator can be taken into account for the analysis.

A scan of the detector perpendicular to the strips in a certain distance from the readout electronics gives the results shown in Fig. 17.

5 Conclusion

This paper introduces the concept of closed MSGC modules proposed for the CMS forward tracker. A prototype was tested in a particle beam and operated at stable cathode voltages well within the efficiency plateau at 97%. During 11 days, no loss of detector performance was observed. The pulse height distribution allows a good separation of signal and noise. No severe variation of the SNR across the wedge shaped strip pattern was found.

Acknowledgements

The authors would like to acknowledge E. Bock, K. Boffin, and D. Jahn (mechanic workshop), H. Liebmann (electric workshop) and Dr. O. Runolfsson, CERN (bonding) for their contributions.

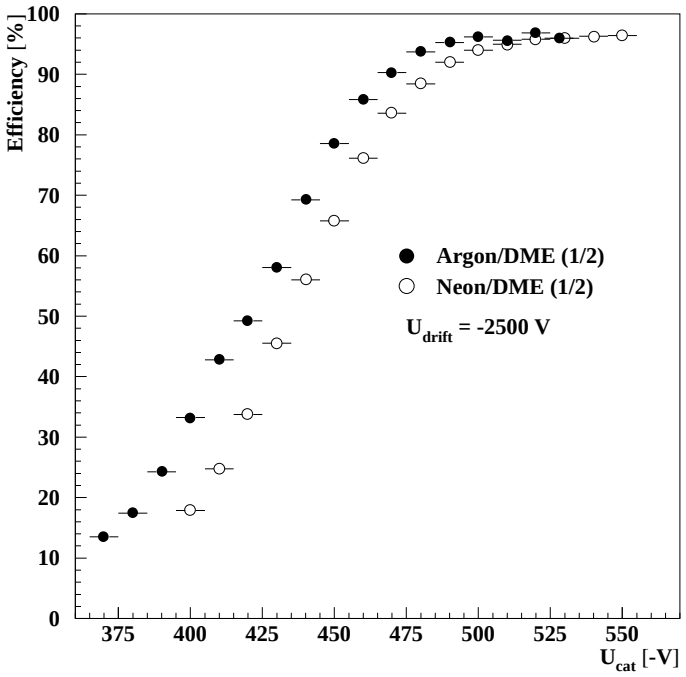

Figure 15: The efficiency plateaus reach absolute values of 97%.

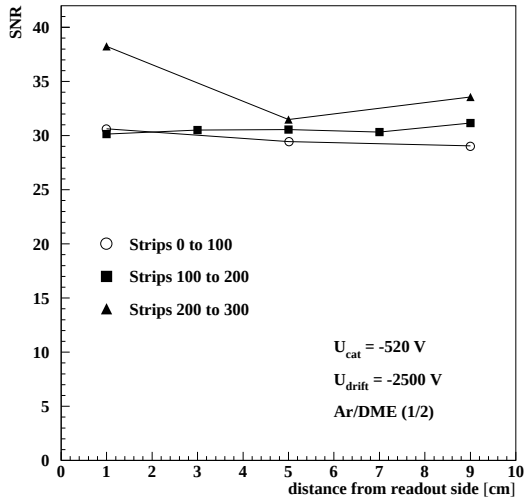

Figure 16: SNR variation along the strips from the readout side (pitch: 200 μm) to the HV side (pitch: 180 μm).

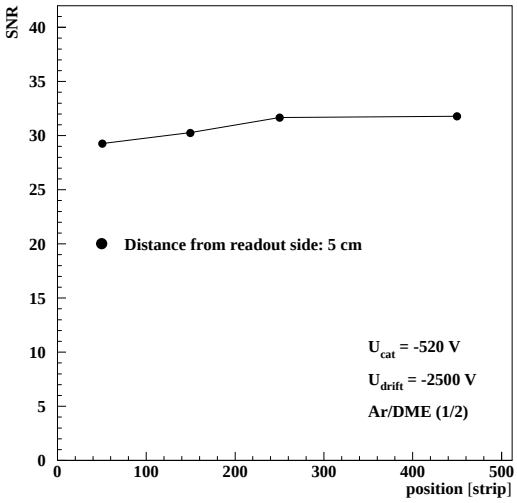

Figure 17: SNR perpendicular to the strips.

References

[1] The Compact Muon Solenoid Technical Proposal, CERN/LHCC 94–38 (December 1994).

[2] A. Oed et al., Position Sensitive Detector with Micro Strip Anode for Electron Multiplication with Gases, Nucl. Instr. and Meth. A 263 (1988) 351.

[3] O. Bouhali et al., A possible approach for the construction of the CMS Forward–Backward MSGC Tracker, Technical Design Report, Inter–University Institute for High Energies (ULB–VUB), Brussels, Belgium (June 1996).

[4] R. Bouclier et al., Ageing of Microstrip Gas Chambers: Problems and Solutions, CERN–PPE/96-33.

[5] L. L. Jones, PreMux128 Specification, version 2.3 (January 1995).

[6] R. Hammarstrøm, CMS Tracker Mother Board (1995).

[7] V. Commichau, PREMUXAD00 V02, III. Physikalisches Institut, RWTH Aachen (January 1996).

[8] V. Commichau, Sequencer SS03 V1, III. Physikalisches Institut, RWTH Aachen (April 1996).

[9] F. Beißel, QUAD FADC V 01 A, III. Physikalisches Institut, RWTH Aachen (April 1996).

[10] M. Petertill, diploma thesis, PITHA 97/23, III. Physikalisches Institut, RWTH Aachen (June 1997).

[11] S. Bachmann et al., Measurements with an MSGC hodoscope using the PreMux128 front–end chip, CMS NOTE 1997/042.

[12] http://nicewww.cern.ch/sl/eagroup/beams.html#x5

[13] J. Kremp, PreMux Electronics Test– and Readout Application (PETRA), User Manual, III. Physikalisches Institut, RWTH Aachen (March 1997).